

A Comparative Normal Table of Anuran Development: Towards a Unified Framework for *Xenopus* and Non-Model Species

Shouhong Wang

wangsh@cib.ac.cn

Chengdu Institute of Biology, Chinese Academy of Sciences

Yanmei Cai

Sichuan Normal University

Zerui Yang

Yibin University

Bin Wang

Chengdu Institute of Biology, Chinese Academy of Sciences

Jianping Jiang

Chengdu Institute of Biology, Chinese Academy of Sciences

Research Article

Keywords: Developmental table, Morphology, Anura, *Xenopus*, *Microhyla fissipes*, *Odorrana tormota*

Posted Date: September 25th, 2025

DOI: <https://doi.org/10.21203/rs.3.rs-7700650/v1>

License:  This work is licensed under a Creative Commons Attribution 4.0 International License.

[Read Full License](#)

Additional Declarations:

Tables 1 and 2 are available in the Supplementary Files section.

No competing interests reported.

1 **A Comparative Normal Table of Anuran Development: Towards a Unified**
2 **Framework for *Xenopus* and Non-Model Species**

3 Shouhong Wang^{a,b}, Yanmei Cai^c, Zerui Yang^d, Bin Wang^{a,b}, Jianping Jiang^{a,b*}

4 ^aMountain Ecological Restoration and Biodiversity Conservation Key Laboratory of
5 Sichuan Province, Chengdu Institute of Biology, Chinese Academy of Sciences,
6 Chengdu, China

7 ^bUniversity of Chinese Academy of Sciences, Beijing, China

8 ^cCollege of Life Science, Sichuan Normal University, Chengdu 610101, China

9 ^dYibin University, Yibin 644000, China

10 ^{*}Corresponding author at: Chengdu Institute of Biology, Chinese Academy of Sciences,
11 Chengdu 610213, China

12 E-mail address: wangsh@cib.ac.cn; jiangjp@cib.ac.cn.

13

14

15

16

17

18

19

20

21

22

23

24

25 **Abstract**

26 **Background** Developmental staging tables, primarily defined by specific external
27 morphological characteristics, are fundamental tools in amphibian research. Although
28 numerous staging tables have been reported for various frog species, significant
29 differences are often observed, especially when compared to the canonical model
30 organism *Xenopus*. To date, no comprehensive study has integrated *Xenopus*
31 developmental stages with the other widely used anuran staging systems, such as the
32 Gosner table.

33 **Results** To bridge this gap, we present the first comparative staging system that directly
34 aligns the *Xenopus* developmental table with two widely used non-model anuran
35 staging systems. This integrated framework was validated through detailed
36 morphological observations across the entire embryonic development of three
37 representative species—*Xenopus laevis/tropicalis*, *Microhyla fissipes*, and *Odorrana*
38 *tormota*—each exemplifying a major staging paradigm. Our system comprehensively
39 covers both early embryonic and postembryonic developmental stages.

40 **Conclusions** This integrated system provides a unified foundation for analyzing
41 morphological development in anurans. It is expected to facilitate cross-species
42 comparisons and promote interdisciplinary research in areas such as ecotoxicology,
43 evolutionary developmental biology, and conservation physiology.

44 **Keywords** Developmental table, Morphology, Anura, *Xenopus*, *Microhyla fissipes*,
45 *Odorrana tormota*

46

47 **Background**

48 Frog amphibians have long served as foundational models in experimental
49 embryology and developmental biology, underpinning many landmark discoveries in
50 the field [1-3]. Their large, robust eggs and embryos are easily accessible for
51 micromanipulation, enabling researchers to gain mechanistic insights into early
52 developmental processes [4-6]. Moreover, the complex biphasic life cycle of most frogs,
53 transitioning from aquatic herbivorous larvae to terrestrial carnivorous adults via
54 metamorphosis, offers a powerful natural system for investigating phenotypic plasticity,
55 cell proliferation, differentiation, and apoptosis [7-11]. Additionally, their permeable
56 skin and dual-phase lifestyle make them highly sensitive bioindicators for assessing
57 environmental toxicity [12].

58 Developmental staging tables are indispensable for standardizing research across
59 laboratories. They provide a temporal framework for understanding morphological
60 transformations, such as cell cleavage patterns, organogenesis (e.g., eyes, limbs, tail),
61 spiracle closure, and tail resorption- and are critical for defining developmental
62 windows and ensuring experimental reproducibility [13, 14]. To date, over 100 anuran
63 species have been documented with species-specific staging tables [15-23]. Although
64 early embryonic and postembryonic development are largely conserved across anurans,
65 significant interspecific variations necessitate the integration of disparate staging
66 systems, especially when comparing non-model species with the well-established
67 *Xenopus* framework.

68 As we know, 3 major staging systems are widely used for describing ontogenetic
69 development in anurans. One is the extensively adopted system created by Gosner
70 (1960), and has been applied in numerous studies [11, 17, 20, 24-28]. This system
71 defines 46 developmental stages based on both external morphological and
72 physiological characteristics, divided into two main phases: 1) early embryonic period
73 (stages G1-25), spanning from fertilization to operculum completion stage; 2) the
74 postembryonic period (G26-46), covering from operculum completion to full tail
75 regression [29, 30]. A second system, similar to that of Gosner, comprises 45
76 developmental stages and likewise includes an early embryonic period (stages S1-28)
77 and a postembryonic phase (S29-45) [8, 22, 31, 32]. In addition, the model organism
78 *Xenopus* has its unique developmental staging system, constructed by Nieuwkoop and
79 Faber (1965). This system encompasses 66 stages from fertilization through complete
80 metamorphosis, also divided into an embryogenesis period (NF1-45) and larval
81 developmental period (NF46-66) [18, 23, 33-35]. A straightforward comparison among
82 these 3 staging systems is a crucial first step toward integrating the developmental
83 timelines of *Xenopus* with non-model anurans, thereby providing a foundation for
84 further comparative and mechanistic research.

85 In this study, we present a detailed comparative developmental table that integrates
86 3 major anuran staging systems, based on detailed morphological observations of
87 *Xenopus laevis/tropicalis*, *Microhyla fissipes*, and *Odorrana tormota*. This unified
88 framework enables precise cross-species staging and uncovers fundamental
89 developmental differences between fully aquatic *Xenopus* and typical anurans, which

90 undergo aquatic-to-terrestrial transitions. By establishing standardized criteria, our
91 work enhances the comparability of developmental research and offers deeper insights
92 into embryological diversity, evolutionary adaptation, and underlying developmental
93 mechanisms.

94 **Materials and methods**

95 **Animal husbandry**

96 Adult *M. fissipes* were collected from farmlands in Shifang City, Sichuan Province,
97 China, while adult *O. tormota* were obtained from Huangshan Hot Springs. Wild-type
98 adults of *X. tropicalis* and *X. laevis* were purchased from NASCO (Fort Atkinson, WI,
99 USA; <http://www.enasco>) and subsequently reared in our laboratory. *M. fissipes* and *O.*
100 *tormota* adults were housed individually in plastic containers (325 mm ×22 mm ×25
101 mm) with moistened sponges to maintain high humidity. Similarly, *Xenopus* adults
102 were maintained in plastic containers with a water depth of 75 mm. All animal
103 procedures were approved by the Animal Care and Use Committee of Chengdu Institute
104 of Biology.

105 **Induced breeding with LHRH-A3 and hCG in frogs**

106 Induced breeding in both male and female *M. fissipes* and *O. tormota* was
107 conducted following standard procedures [22]. Briefly, each frog received a single
108 intraperitoneal injection of luteinizing hormone-releasing hormone A3 (LHRH-A3) at
109 a dosage of 0.3 µg/g body weight. For sexually mature *X. tropicalis* and *X. laevis*, an
110 initial priming injection of 20 U of human chorionic gonadotropin (hCG) was
111 administered on day 1. The following day, males and females of both *Xenopus* received

112 subsequent hCG boosts: males administered 200 U, while females received 250 U for
113 *X. tropicalis* and 650 U for *X. laevis*, respectively.

114 **Tadpole feeding and observation during embryonic development**

115 Fertilized embryos were collected and placed into larger plastic containers (325
116 mm × 405 mm × 115 mm; water depth: 80 mm) for rearing. Tadpoles were maintained
117 at a temperature of 25 ± 0.5 °C under a 12:12 hour light/dark cycle. All tadpoles were
118 fed spirulina powder (China National Salt Industry Corporation) twice daily, and the
119 water was replaced every two days. Developmental stages of *O. tormota*, *M. fissipes*,
120 and *Xenopus* were determined based on the staging tables reported by Gosner (1960),
121 Wang et al. (2017) and Nieuwkoop and Faber (1965), respectively. Morphological
122 characteristics of the tadpoles and the photographs of each animal were acquired using
123 a stereo microscope (JSZ8T, Jiang Nan Yong Xin, Nanjing, China) equipped with the
124 Mshot Image Analysis system (Mc50-N).

125 **Results**

126 **Early embryonic development stage**

127 The early embryonic development period of anurans is often described from the
128 zygote formation to the operculum completion (G1/S1/NF1-G25/S28/NF45). This
129 period encompasses several distinct stages, including fertilization, cleavage, blastula
130 formation, gastrulation, neurulation, tail elongation, eye development, gill development,
131 and the formation of the spiracle (Table 1).

132 **Zygote and cleavage stage**

133 Shortly after fertilization, the egg undergoes rotation, with the darkly pigmented

134 animal hemisphere moving to the upper side while the lighter vegetal hemisphere faces
135 downward. The cleavage phase is commonly characterized by the number of cells,
136 spanning from the 2-cell stage (G3/S3/NF2) to 32-cell stage (G7/S7/NF6). In contrast,
137 the blastula phase is typically distinguished based on cell size (Table 1, Fig.1).

138 Most anuran species, such as *Xenopus*, *M. fissipes*, and *O. tormota*, exhibit a
139 “standard” cleavage pattern. This pattern is defined by the first two cleavages being
140 meridional, followed by a third latitudinal cleavage, and then an extensive series of
141 synchronous divisions in the animal hemisphere (Fig.1 A1-C1).

142 **Gastrula and neurula stage**

143 The onset of gastrula stage (G10/S11/NF9-G12/S14/NF11-13) is characterized by
144 blastopore formation, followed by dynamic changes in its size and shape (Table 1,
145 Fig.1A2-C2). During the late gastrula stage (G12/S14/NF11-13), the yolk plug
146 disappears, resulting in a horseshoe-shaped embryo (Table 1). Subsequent neural stages
147 are marked by the sequential development of the neural plate (G13/S15/NF14), the
148 elevation of neural folds (G14/S16/NF15-17), and the closure of the neural tube
149 (G16/S18/NF19-21) (Table 1, Fig.1A3-C3).

150 **Embryo and organogenesis stage**

151 During the embryo and organogenesis stages, key morphological structures
152 emerge sequentially. A tail bud becomes visible at the posterior end, followed by the
153 formation of a gray eye cup and progressive tail elongation around stages G17-18/S19-
154 21/NF22-32 (Table 1, Fig. 1A4-C4). Notably, a heartbeat is first detectable at
155 G19/S22/NF33-34. Subsequently, gill buds appear and expand, coinciding with embryo

156 hatching (G20/S23/NF35-36). During this period, developmental staging can also be
157 assessed using intestinal morphology. For example, by G24/S26/NF44, the intestine
158 develops a distinct S-shaped loop (Fig. 1A5-C5). Finally, the operculum subsequently
159 forms, enveloping the gill buds and completing spiracle formation. This stage marks
160 the onset of feeding and the transition to free-swimming tadpoles (Table 1, Fig.1 A5-
161 C5).

162 **Postembryonic development stage**

163 Generally, the postembryonic development period, spanning from hindlimb bud
164 emergence to tail resorption (G26/S29/NF48-G46/S45/NF66), is characterized by
165 series of morphological transformations. These include limb bud development,
166 hindlimb growth, toes differentiation and growth, head reshaping, and ultimately tail
167 resorption. It should be noted that the endpoint of this period differs between species.
168 In *Xenopus*, it concludes at the end of metamorphosis (NF66), whereas in most other
169 anurans, it is defined by the complete disappearance of the tail (G46/S45) (Table 2).

170 **Limb development and growth**

171 Tadpoles at G26/S29/NF48 are clearly identified by the presence of gold
172 iridophores around the gut and the emergence of hindlimb buds (Table 2, Fig.2A1-
173 C1). Subsequent developmental stages from G27/S30/NF49 to G29/S32/NF51 are
174 readily determined by the length/width ratio of the hindlimb bud. For instance, by
175 G28/S31/NF50, the hindlimb bud length equals its width (Table 2). Additionally, the
176 hindlimb bud exhibits an oar-shaped outline of the foot by G31/S33/NF52.

177 Next, from G32/S34/NF53 to G36/S36/NF54, developmental staging is
178 determined by the degree of toe differentiation. The process begins at G32/S34/NF53
179 and completes at G36/S36/NF54, when all five toes are fully distinct (Table 2, Fig.A2-
180 C2; Fig.A3-C3). This phase represents a key transition from pre- to pro-
181 metamorphosis.

182 Further stages can be identified through toe morphology, including the
183 appearance of metatarsal and subarticular tubercles. By G40/S40/NF58, tadpoles
184 reach their maximum body and tail length. In *Xenopus*, forelimbs erupt from the
185 ventral skin at this stage (NF58) (Table 2).

186 **Tail resorption and head reshaping**

187 These stages represent the transition from the climax of metamorphosis to the end
188 of metamorphosis (G40/S40/NF58-G46/S45/NF66) (Table 2, Fig. 3). During this
189 period, tail resorption and head narrowing occur progressively. Tail resorption initiates
190 around G42/S42/NF60-61, accompanied by a slight reduction in tail length and
191 narrowing of the head, coinciding with near-peak plasma T3 levels.

192 By G43/S42-43/NF62, around 2/3 of the tail is resorbed. Additionally, the head
193 becomes narrower than the trunk, while the tail remains slightly longer than the body.
194 In most anuran species except *Xenopus*, forelimbs erupt from the ventral skin at this
195 stage (S42/G42) (Fig. 3B2-C2). Next, rapid tail resorption occurs between
196 G44/S43/NF63 and G46/S45/NF66, eventually in the completion of metamorphosis
197 and the formation of a tailless frog.

198 **Discussion**

199 In this study, we established the first integrated and comprehensive staging system
200 that combines 3 major anuran developmental systems: the widely used Gosner (G)
201 stages (G1-66), a second key anuran staging system (S1-45), and the classic Nieuwkoop
202 and Faber (NF) Normal Table for the model species *Xenopus* (NF1-66). Our
203 comprehensive framework covers both early embryonic (G1/S1/NF1-G25/S28/NF45)
204 and postembryonic (G26/S29/NF48-G46/S45/NF66) development, where the aquatic
205 tadpoles undergo metamorphosis into a juvenile frog [17, 18, 22]. This integrated
206 framework offers a standardized and efficient tool for accurate developmental staging
207 across diverse anuran species, offering a critical reference for ecological, conservation,
208 and experimental studies where accurate and consistent developmental staging is
209 crucial.

210 **Larval period: rapid and efficient organization provides essential materials for**
211 **researching organ development**

212 Early tadpole development, characterized by external fertilization, cleavage,
213 neurulation, tail elongation, eye development, is a rapid, complex, and tightly regulated
214 process, exhibiting distinct stage-specific characteristics that render them highly
215 valuable as developmental biology models [36-38]. Developmental time courses,
216 however, varies among different species. For example, it takes around 20 minutes in
217 *Xenopus* and 10 minutes in *M. fissipes* at 25°C to complete the fertilization [22, 39].
218 Embryonic development lasts 3-4 days in *X. tropicalis* at 25°C, compared to 4 days in
219 *X. laevis* at 20°C [18, 34]. *M. fissipes* requires around 70 hours at 24-26°C, whereas
220 *Kaloula borealis* completes embryogenesis in just 30 hours at room temperature [20,

221 22]. Yet, some species, such as those in the family Megophryidae, exhibit markedly
222 prolonged early embryonic development; for example, *Vibrissaphora leishanensis*
223 takes approximately 116 days (2,784 hours) at 6.3–11.5°C [40]. This diversity in
224 developmental timing is fascinating and may represent a significant aspect of the
225 evolutionary embryology.

226 At the single-cell embryo stage (G1/S1/NF1), techniques such as microinjection
227 and fluorescence labeling enable highly efficient gene knockout or knockin [41-43],
228 allowing precise functional genetic manipulation via targeted inhibition or
229 overexpression. After fertilization, rapid cell divisions (cleavage) occur without an
230 increase in overall egg volume, offering a powerful model for investigating the
231 mechanisms and regulation of early mitotic cycles. In addition, these stages serve as
232 models to assess the impact of external factors (e.g., temperature, chemical exposure)
233 on cell division [32, 44]. Subsequent gastrulation is a fundamental process of metazoan
234 embryogenesis, during which germ layers are formed through extensive cell
235 movements and differentiation [45, 46]. Importantly, as the neural tube eventually
236 develops into the central nervous system, including the brain and spinal cord, “Neural
237 stages” (G13-16/S15-18/NF14-21) are crucial for studying early neurodevelopment [47,
238 48].

239 Once the neural tube has formed, it induces changes in its neighbors, and
240 organogenesis continues [49]. The initiation of tail bud (G17/S19/NF22-25) provides a
241 suitable window for investigating tail development and regeneration [6, 34, 50]. For
242 example, Wang et al. (2021) showed that the tail could fully regenerative from the tail

243 bud stage to the onset of metamorphosis climax (NF60/61) except for a refractory
244 period (NF45-47), which temporarily lost the regenerative ability in *X. laevis* [34, 51,
245 52]. This regenerative transition offers a useful model to deciphering molecular
246 mechanisms governing regeneration competence.

247 In addition, by the tadpole stage, gill development supports efficient oxygen
248 exchange, enabling locomotion and feeding [53]. This period is marked by active
249 organogenesis, with upregulated expression of genes essential for the development and
250 functional maturation of the heart, liver, kidneys, and other organs [32, 54]. Their
251 transparency, permeable skin, and aquatic lifestyle of tadpoles also make them ideal for
252 toxicological and environmental studies [55-57]. For example, Chen et al. (2025)
253 examined triclosan-induced neurotoxicity in *Rana omeimontis* tadpoles (G22) [57],
254 while Chai et al. (2023) explored heavy metals effects in *Bufo gargarizans* tadpoles
255 (G26-38) [58]. Overall, frog larval development is an ideal and essential model for
256 developmental, evolutionary, and conservation studies, as it is an independent process
257 that is not influenced by maternal factors and develops rapidly.

258 **Metamorphosis: an evolutionary transition from aquatic to terrestrial life**

259 Frog metamorphosis is a postembryonic process marked by dramatic
260 morphological changes, including de novo organ formation (such as limbs), remodeling
261 of existing organs (including the intestine, brain, and pancreas) and regression of larval
262 structures (e.g., gills and tail) [9, 59]. This fascinating event in frogs is primarily
263 orchestrated by thyroid hormone (TH) via precise gene regulatory mechanisms [8, 60].
264 Thus, amphibian metamorphosis provides us with an excellent model for understanding

265 the fundamental mechanisms that govern postembryonic organ development and
266 programmed tissue remodeling.

267 Numerous studies have been carried out in frogs during the post-embryonic
268 development period, especially during the metamorphosis stage. There are a number of
269 similarities between anuran metamorphosis and postembryonic development in
270 mammals, including thyroid hormone secretion, organ maturation, tissue regression, a
271 switch from fetal or larval to adult hemoglobin, and the transition from aquatic to a
272 terrestrial environment (from uterus to delivery) [8, 53, 60-64]. Understanding these
273 conserved developmental events in frogs can thus provide insights into human
274 developmental disorders.

275 **Frogs as model organisms for organ regeneration**

276 Elucidating how to promote organ and appendage regeneration is a major goal of
277 regenerative medicine [65]. Intriguingly, many frog organs, such as tail, heart, brain,
278 and spinal cord, can achieve both scar-free healing and tissue regeneration during their
279 larval stages, while this ability declines during metamorphosis as TH level rise [10, 33,
280 65, 66]. In addition, elevated TH levels have been reported to inhibit appendage
281 regeneration, such as heart and tail [67, 68]. For example, Marshall et al. (2019)
282 revealed that both TH excess and natural peaks during metamorphosis disrupt heart
283 regeneration in *Xenopus*, altering fibrotic responses and extracellular matrix gene
284 expression [33]. Concurrently, we and others have observed substantial cardiac
285 remodeling during metamorphic climax (Additional file 1) [33, 69], including chamber
286 separation, cardiomyocytes mature, and a decline in regenerative capacity. It remains

287 unclear whether these structural changes influence the cardiomyocyte dedifferentiation
288 and impair regenerative ability [70]. Interestingly, neonatal mammals also exhibit
289 transient cardiac regenerative potential that is lost postnatally as TH levels increase
290 [71,72], suggesting an evolutionarily conserved role for TH in modulating tissue
291 regeneration. Investigating the TH-mediated loss of regenerative capacity in frogs may
292 therefore yield novel insights for regenerative medicine.

293 **Conclusion**

294 In summary, the integrated staging system proposed in this study establishes a
295 robust and unified framework for comparative developmental research in anurans,
296 facilitating more precise cross-species analyses between *Xenopus* and non-model frogs.
297 By systematically aligning staging tables and morphological characteristics, our work
298 uncovers both conserved developmental patterns and species-specific adaptations.
299 Anuran embryonic development, including both early embryonic and postembryonic
300 development, emerges as a powerful and independent model for investigating
301 fundamental questions in developmental biology, evolution, regeneration, toxicology,
302 and environmental adaptation. Importantly, we highlight the use of diverse frog
303 species—not just the established model *Xenopus*—in molecular, cellular, toxicological,
304 and evolutionary investigations. Future applications of advanced methods such as
305 micro-CT, molecular profiling, and single-cell technologies will further elucidate the
306 conserved and unique mechanisms underlying anuran development, supporting future
307 discoveries in basic and translational science.

308 **Availability of data and materials**

309 All data generated or analysed during this study are included in this published article.

310 **Competing interests**

311 The authors declare no competing interests.

312 **Funding**

313 This work was supported by the National Natural Science Foundation of China (Grant
314 No. 3240030299), the Natural Science Foundation of Sichuan Province of China (Grant
315 No. 2024NSFSC1183), and the International Partnership Program of the Chinese
316 Academy of Sciences (For Future Network; Grant No. 069GJHZ2024053FN).

317 **Authors' contributions**

318 **Shouhong Wang:** Writing–original draft, Writing–review & editing, Methodology,
319 Investigation, Funding acquisition, Data curation, Conceptualization. **Yanmei Cai:**
320 Data curation, Writing – review & editing. **Zerui Yang:** Data curation, Writing–review
321 & editing. **Bin Wang:** Writing–review & editing, Supervision. **Jianping Jiang:** Writing
322 – review & editing, Supervision.

323 **Acknowledgements**

324 The graphical abstract was created using BioRender. com.

325 **References**

- 326 1. Morgan TH: The development of the frog's egg: an introduction to experimental
327 embryology: Macmillan; 1897.
- 328 2. De Robertis EM, Gurdon JB: A brief history of *Xenopus* in biology. Cold Spring
329 Harb Protoc. 2021; 12: pdb. top107615.
- 330 3. Lania G, Schnabel D, Schubert M: Model organisms in embryonic development.
331 In., vol. 13: Fron Cell Dev Biol. 2025; 1649186.
- 332 4. Beck CW, Slack JMW: An amphibian with ambition: a new role for *Xenopus* in
333 the 21st century. Genome Biol. 2001; 2(10).
- 334 5. Yergeau DA, Mead PE: Manipulating the *Xenopus* genome with transposable
335 elements. Genome Biol. 2007; 8:1-11.
- 336 6. Wang S, Liu L, Shi YB, Jiang J: Transcriptome profiling reveals gene regulation

- 337 programs underlying tail development in the Ornamented Pygmy frog
338 *Microhyla fissipes*. Front Biosci (Landmark Ed). 2021; 26:1001-1012.
- 339 7. Wen L, Shibata Y, Su D, Fu L, Luu N, Shi YB: Thyroid Hormone Receptor
340 alpha Controls Developmental Timing and Regulates the Rate and Coordination
341 of Tissue-Specific Metamorphosis in *Xenopus tropicalis*. Endocrinology. 2017;
342 158:1985-1998.
- 343 8. Wang S, Liu L, Liu J, Zhu W, Tanizaki Y, Fu L, Bao L, Shi Y-B, Jiang J: Gene
344 expression program underlying tail resorption during thyroid hormone-
345 dependent metamorphosis of the ornamented pygmy frog *Microhyla fissipes*.
346 Front Endocrinol. 2019; 10:11.
- 347 9. Shi YB: Life Without Thyroid Hormone Receptor. *Endocrinology* 2021, 162(4).
- 348 10. Wang S, Shibata Y, Fu L, Tanizaki Y, Luu N, Bao L, Peng Z, Shi Y-B: Thyroid
349 hormone receptor knockout prevents the loss of *Xenopus* tail regeneration
350 capacity at metamorphic climax. Cell Biosci. 2023; 13:1-14.
- 351 11. Lu N, Zhu W, Tang C-Y, Yan C, Chen Q, Wu W, Chang L, Jiang J, Li J-T, Wang
352 B: Genome of a stage-dependent cave-dwelling frog reveals the genetic
353 mechanism of an extremely divergent biphasic life cycle. Cell Re. 2025; 44:
354 115640-115662.
- 355 12. Lv Y, Zhang Q-D, Chang L-M, Yang D-L, Riaz L, Li C, Chen X-H, Jiang J-P,
356 Zhu W: Multi-omics provide mechanistic insight into the Pb-induced changes
357 in tadpole fitness-related traits and environmental water quality. Ecotoxicol
358 Environ Saf. 2022; 247:114207-114219.
- 359 13. Hopwood N: A history of normal plates, tables and stages in vertebrate
360 embryology. Int J Dev Biol. 2007; 51:1-26.
- 361 14. Parichy DM, Elizondo MR, Mills MG, Gordon TN, Engeszer RE: Normal table
362 of postembryonic zebrafish development: staging by externally visible anatomy
363 of the living fish. Dev Dyn. 2009; 238:2975-3015.
- 364 15. Shumway W: Stages in the normal development of *Rana pipiens* I. External
365 form. Anat Rec. 1940; 78:139-147.
- 366 16. Taylor AC, Kollros JJ: Stages in the Normal Development of *Rana-Pipiens*
367 Larvae. Anat Rec. 1946; 94:7-23.
- 368 17. Gosner KL: A simplified table for staging anuran embryos and larvae with notes
369 on identification. Herpetologica. 1960; 16:183-190.
- 370 18. Nieuwkoop PD, Faber J: Normal table of *Xenopus laevis*. 1965.
- 371 19. Ba-Omar T, Ambu-Saidi I, Al-Bahry S, Al-Khayat AJZitME: Embryonic and
372 larval staging of the Arabian Toad, *Bufo arabicus* (Amphibia: Bufonidae).
373 Zoology in the Middle East. 2004; 32:47-56.
- 374 20. Xiong R-C, Jiang J-P, Liang F, Wang B, Ye C-Y: Embryonic development of the
375 concave-eared torrent frog with its significance on taxonomy. Zool Res. 2011;
376 490-498.
- 377 21. Araujo OG, Haddad CF, Silva HR, Pugener LA: A simplified table for staging
378 embryos of the pipid frog *Pipa arrabali*. An Acad Bras Cienc. 2016; 88:1875-
379 1887.
- 380 22. Wang SH, Zhao LY, Liu LS, Yang DW, Khatiwada JR, Wang B, Jiang JP: A

- 381 Complete Embryonic Developmental Table of *Microhyla fissipes* (Amphibia,
382 Anura, Microhylidae). Asian Herpetol Res. 2017; 8:108-117.
- 383 23. Zahn N, James-Zorn C, Ponferrada VG, Adams DS, Grzymkowski J, Buchholz
384 DR, Nascone-Yoder NM, Horb M, Moody SA, Vize PD: Normal Table of
385 *Xenopus* development: a new graphical resource. Development. 2022;
386 149:dev200356.
- 387 24. Grenat PR, Gallo LMZ, Salas NE, Martino AL: External changes in embryonic
388 and larval development of *Odontophrynus cordobae* Martino et Sinsch, 2002
389 (Anura: Cycloramphidae). Biologia. 2011; 66:1148-1158.
- 390 25. Simmons AM: Tadpole bioacoustics: Sound processing across metamorphosis.
391 Behav Neurosci. 2019; 133:586-601.
- 392 26. Salla RF, Gamero FU, Rissoli RZ, Dal-Medico SE, Castanho LM, Carvalho
393 Cdos S, Silva-Zacarin EC, Kalinin AL, Abdalla FC, Costa MJ: Impact of an
394 environmental relevant concentration of 17alpha-ethinylestradiol on the cardiac
395 function of bullfrog tadpoles. Chemosphere. 2016; 144:1862-1868.
- 396 27. Garcia-Munoz E, Guerrero F, Bicho RC, Parra G: Effects of ammonium nitrate
397 on larval survival and growth of four Iberian amphibians. Bull Environ Contam
398 Toxicol. 2011; 87:16-20.
- 399 28. Sayim F, Kaya U: Embryonic development of the tree frog, *Hyla arborea*.
400 Biologia. 2008; 63:588-593.
- 401 29. Bowatte G, Meegaskumbura MJA, conservation r: Morphology and ecology of
402 *Microhyla rubra* (Anura: Microhylidae) tadpoles from Sri Lanka. Amphib
403 Rrptile Conse. 2011; 5:22-32.
- 404 30. Behr N, Rödder D: Larval development stages and husbandry of the Rice Frog
405 *Microhyla mukhlesuri* Hasan et al., 2014 (Anura: Microhylidae). Bonn Zool
406 Bull. 2018; 67: 109-116.
- 407 31. Shimizu S, Ota HJCh: Normal Development of *Microhyla ornata*. Curr
408 Herpetol. 2003; 22:73-90.
- 409 32. Lu-Sha L, Lan-Ying Z, Shou-Hong W: Research proceedings on amphibian
410 model organisms. Zool Res. 2016; 37:237.
- 411 33. Marshall LN, Vivien CJ, Girardot F, Pericard L, Scerbo P, Palmier K, Demeneix
412 BA, Coen L: Stage-dependent cardiac regeneration in *Xenopus* is regulated by
413 thyroid hormone availability. Proc Natl Acad Sci. 2019; 116:3614-3623.
- 414 34. Wang S, Shi Y-B: Evolutionary divergence in tail regeneration between
415 *Xenopus laevis* and *Xenopus tropicalis*. Cell Biosci. 2021; 11:1-4.
- 416 35. Sindelka R, Naraine R, Abaffy P, Zucha D, Kraus D, Netusil J, Smetana Jr K,
417 Lacina L, Endaya BB, Neuzil J: Characterization of regeneration initiating cells
418 during *Xenopus laevis* tail regeneration. Genome Biol. 2024; 25:251.
- 419 36. Thomsen GH: A new century of amphibian developmental biology. Semin Cell
420 Dev Biol. 2006; 17:78-79.
- 421 37. Shangpliang PW, Shadap R, Hooroo RNK, Nongkynrih SJ, Kharkongor M,
422 Rangad D, Tron RKL: The First Comprehensive Description of the Normal
423 Development of Annandale's High Altitude Frog, *Kurixalus naso* (Annandale,

- 1912). *Curr Herpetol.* 2021; 40:137-150.
- 425 38. Chuliver M, Agnolín FL, Scanferla A, Aranciaga Rolando M, Ezcurra MD,
426 Novas FE, Xu X: The oldest tadpole reveals evolutionary stability of the anuran
427 life cycle. *Nature.* 2024; 636:138-142.
- 428 39. Shibata Y, Bao L, Fu L, Shi B, Shi Y-B: Functional studies of transcriptional
429 cofactors via microinjection-mediated gene editing in *Xenopus*. In:
430 *Microinjection: Methods and Protocols.* Springer; 2018: 507-524.
- 431 40. Chen J, Pan C, Wang Y, Yao L, Yang S: A Preliminary Study on the
432 Reproduction Ecology for *Vibrissaphora leishanensis*. *Sichuan J Zool.* 2017;
433 36:4 (In Chinese with English Abstract).
- 434 41. Nakajima K, Tazawa I, Yaoita Y: Thyroid Hormone Receptor alpha- and beta-
435 Knockout *Xenopus tropicalis* Tadpoles Reveal Subtype-Specific Roles During
436 Development. *Endocrinology.* 2018; 159:733-743.
- 437 42. Chen S, Jiao Y, Pan F, Guan Z, Cheng SH, Sun D: Knock-in of a large reporter
438 gene via the high-throughput microinjection of the CRISPR/Cas9 system. *IEEE*
439 *Trans Biomed Eng.* 2022; 69:2524-2532.
- 440 43. Shibata Y, Suzuki M, Hirose N, Takayama A, Sanbo C, Inoue T, Umesono Y,
441 Agata K, Ueno N, Suzuki K-iT: CRISPR/Cas9-based simple transgenesis in
442 *Xenopus laevis*. *Dev Bio.* 2022; 489:76-83.
- 443 44. Ishihara K, Nguyen PA, Wühr M, Groen AC, Field CM, Mitchison TJ:
444 Organization of early frog embryos by chemical waves emanating from
445 centrosomes. *Philos Trans R Soc B Biol Sci.* 2014; 369:20130454.
- 446 45. Nájera GS, Weijer CJ: The evolution of gastrulation morphologies.
447 *Development.* 2023; 150: dev200885.
- 448 46. Gilbert SF: “When does human life begin?” teaching human embryology in the
449 context of the American abortion debate. *Dev Biol.* 2024; 515:102-111.
- 450 47. Greene ND, Copp AJ: Development of the vertebrate central nervous system:
451 formation of the neural tube. *Prenat Diagn.* 2009; 29:303-311.
- 452 48. del Pino EM, Venegas-Ferrín M, Romero-Carvajal A, Montenegro-Larrea P,
453 Sáenz-Ponce N, Moya IM, Alarcón I, Sudou N, Yamamoto S, Taira M: A
454 comparative analysis of frog early development. *Proc Natl Acad Sci.* 2007;
455 104:11882-11888.
- 456 49. Gilbert SF: *Developmental biology.* In.: Sinauer associates; 2000.
- 457 50. Beck CW, Slack JM: Analysis of the developing *Xenopus* tail bud reveals
458 separate phases of gene expression during determination and outgrowth. *Mech*
459 *Dev.* 1998; 72:41-52.
- 460 51. Beck CW, Christen B, Slack JMW: Molecular pathways needed for regeneration
461 of spinal cord and muscle in a vertebrate. *Dev Cell.* 2003; 5:429-439.
- 462 52. Aztekin C, Hiscock TW, Marioni JC, Gurdon JB, Simons BD, Jullien J:
463 Identification of a regeneration-organizing cell in the *Xenopus* tail. *Science.*
464 2019; 364:653-658.
- 465 53. Chang L, Zhu W, Jiang J: What frog gill resorption brings: loss of function, cell
466 death, and metabolic reorganization. *Front Zool.* 2024; 21:11.
- 467 54. Carotenuto R, Pallotta MM, Tussellino M, Fogliano C: *Xenopus laevis* (Daudin,

- 468 1802) as a model organism for bioscience: a historic review and perspective.
469 Biology. 2023; 12:890.
- 470 55. Zhu W, Zhang M, Chang L, Zhu W, Li C, Xie F, Zhang H, Zhao T, Jiang J:
471 Characterizing the composition, metabolism and physiological functions of the
472 fatty liver in *Rana omeimontis* tadpoles. Front Zool. 2019; 16:1-17.
- 473 56. Chang L, Wang B, Zhang M, Liu J, Zhao T, Zhu W, Jiang J: The effects of
474 corticosterone and background colour on tadpole physiological plasticity. Comp
475 Biochem Physiol Part D Genomics Proteomics. 2021; 39:100872.
- 476 57. Chen G, Xia X, Xie J, Cao Y, Yuan C, Yu G, Wei S, Duan Y, Cai Y, Wang S:
477 Dose-dependent toxic effects of triclosan on *Rana omeimontis* larvae: Insights
478 into potential implications for neurodegenerative diseases. J Hazard Mater.
479 2025; 487:137187.
- 480 58. Zhang S, Chen A, Jiang L, Liu X, Chai L: Copper-mediated shifts in
481 transcriptomic responses of intestines in *Bufo gargarizans* tadpoles to lead stress.
482 Environ Sci Pollut Res Int. 2023; 30:50144-50161.
- 483 59. Nizam KS, Ismail NA, Farinordin FA, Izam NAM: Frog Metamorphosis: A
484 Review of Metamorphic Stages, Developmental Progression, and Influential
485 Factors. Bioresour Environ. 2023;1:120-155.
- 486 60. Shibata Y, Wen L, Okada M, Shi YB: Organ-Specific Requirements for Thyroid
487 Hormone Receptor Ensure Temporal Coordination of Tissue-Specific
488 Transformations and Completion of *Xenopus* Metamorphosis. Thyroid. 2020;
489 30:300-313.
- 490 61. Buchholz DR: More similar than you think: Frog metamorphosis as a model of
491 human perinatal endocrinology. Dev Biol. 2015; 408:188-195.
- 492 62. Shibata Y, Tanizaki Y, Shi YB: Thyroid hormone receptor beta is critical for
493 intestinal remodeling during *Xenopus tropicalis* metamorphosis. Cell Biosci.
494 2020; 10:46.
- 495 63. Tanizaki Y, Shibata Y, Zhang H, Shi YB: Analysis of Thyroid Hormone
496 Receptor alpha-Knockout Tadpoles Reveals That the Activation of Cell Cycle
497 Program Is Involved in Thyroid Hormone-Induced Larval Epithelial Cell Death
498 and Adult Intestinal Stem Cell Development During *Xenopus tropicalis*
499 Metamorphosis. Thyroid. 2021; 31:128-142.
- 500 64. Chang L, Chen Q, Wang B, Liu J, Zhang M, Zhu W, Jiang J: Single cell RNA
501 analysis uncovers the cell differentiation trajectories and functionalization for
502 air breathing of frog lung. Commun Biol. 2024; 7:665.
- 503 65. Phipps LS, Marshall L, Dorey K, Amaya E: Model systems for regeneration:
504 *Xenopus*. Development. 2020; 147: dev180844.
- 505 66. Lee-Liu D, Méndez-Olivos EE, Muñoz R, Larraín J: The African clawed frog
506 *Xenopus laevis*: a model organism to study regeneration of the central nervous
507 system. Neurosci Lett. 2017; 652:82-93.
- 508 67. Hirose K, Payumo AY, Cutie S, Hoang A, Zhang H, Guyot R, Lunn D, Bigley
509 RB, Yu H, Wang J: Evidence for hormonal control of heart regenerative capacity
510 during endothermy acquisition. Science. 2019; 364:184-188.
- 511 68. Wang S, Fu L, Wang B, Cai Y, Jiang J, Shi Y-B: Thyroid hormone receptor-and

512 stage-dependent transcriptome changes affect the initial period of *Xenopus*
513 *tropicalis* tail regeneration. BMC Genomics. 2024; 25:1260.

514 69. Lv L, Guo W, Guan W, Chen Y, Huang R, Yuan Z, Pu Q, Feng S, Zheng X, Li
515 Y: Echocardiographic assessment of *Xenopus tropicalis* heart regeneration. Cell
516 Biosci. 2023; 13:29.

517 70. Beisaw A, Wu CC: Cardiomyocyte maturation and its reversal during cardiac
518 regeneration. Dev Dyn. 2024; 2531:8-27.

519 71. Porrello ER, Mahmoud AI, Simpson E, Hill JA, Richardson JA, Olson EN,
520 Sadek HA: Transient regenerative potential of the neonatal mouse heart.
521 Science. 2013; 31:1078-1080.

522 72. Wang J, An M, Haubner BJ, Penninger JM: Cardiac regeneration: Options for
523 repairing the injured heart. Front in Cardiovasc Med. 2023; 9:981982.

524
525
526
527
528
529
530
531
532
533
534
535
536
537
538
539
540
541
542
543
544
545

546 **Figure Legends**

547 **Fig.1** The comparison analysis of representative embryonic developmental stages
548 across 3 species: (A) *Xenopus*, (B) *Microhyla fissipes*, and (C) *Odorrana tormotus*;
549 (A1-C1) Cleavage stages; (A2-C2) Gastrula stage; (A3-C3) Neurula stage; (A4-C4)
550 Tail development; and (A5-C5) Operculum formation. Red arrows (a) show the
551 development of optic vesicles, while red arrows (b) indicate tail bud development. Scale
552 bars are 0.5 mm (A1-C4) and 2 mm (A5-C5).

553 **Fig.2** The comparison analysis of representative limb bud developmental stages across
554 3 species: (A) *Xenopus*, (B) *Microhyla fissipes*, and (C) *Odorrana tormotus*; (A1-C1)
555 Appearance of limb bud; (A2-C2) Development of limb bud; (A3-C3) Toe
556 differentiation. Red arrows show the magnification of limb buds or differentiated toes.
557 Scale bars are 2 mm.

558 **Fig.3** Tail resorption stages in *Xenopus* (A), *Microhyla fissipes* (B), and *Odorrana*
559 *tormotus*(C). (A1-C1) Eruption of forelimbs (dorsal view); (A2-C2) Tail resorptions at
560 metamorphosis climax (dorsal view); (A3-C3) Completion of metamorphosis (dorsal
561 view). Scale bars are 2 mm.

562 **Table Legends**

563 **Table 1.** Comparison of early embryonic development among the major 3 staging tables,
564 including Goner (1960) for most anurans, Wang (2017) for *Microhyla fissipes*, and
565 Nieuwkoop and Faber (1956) for the model species *Xenopus*.

566 **Table 2.** Comparison of post-embryonic development among the major 3 staging tables,
567 including Goner (1960) for most anurans, Wang (2017) for *Microhyla fissipes*, and
568 Nieuwkoop and Faber (1956) for the model species *Xenopus*.

569

Figures

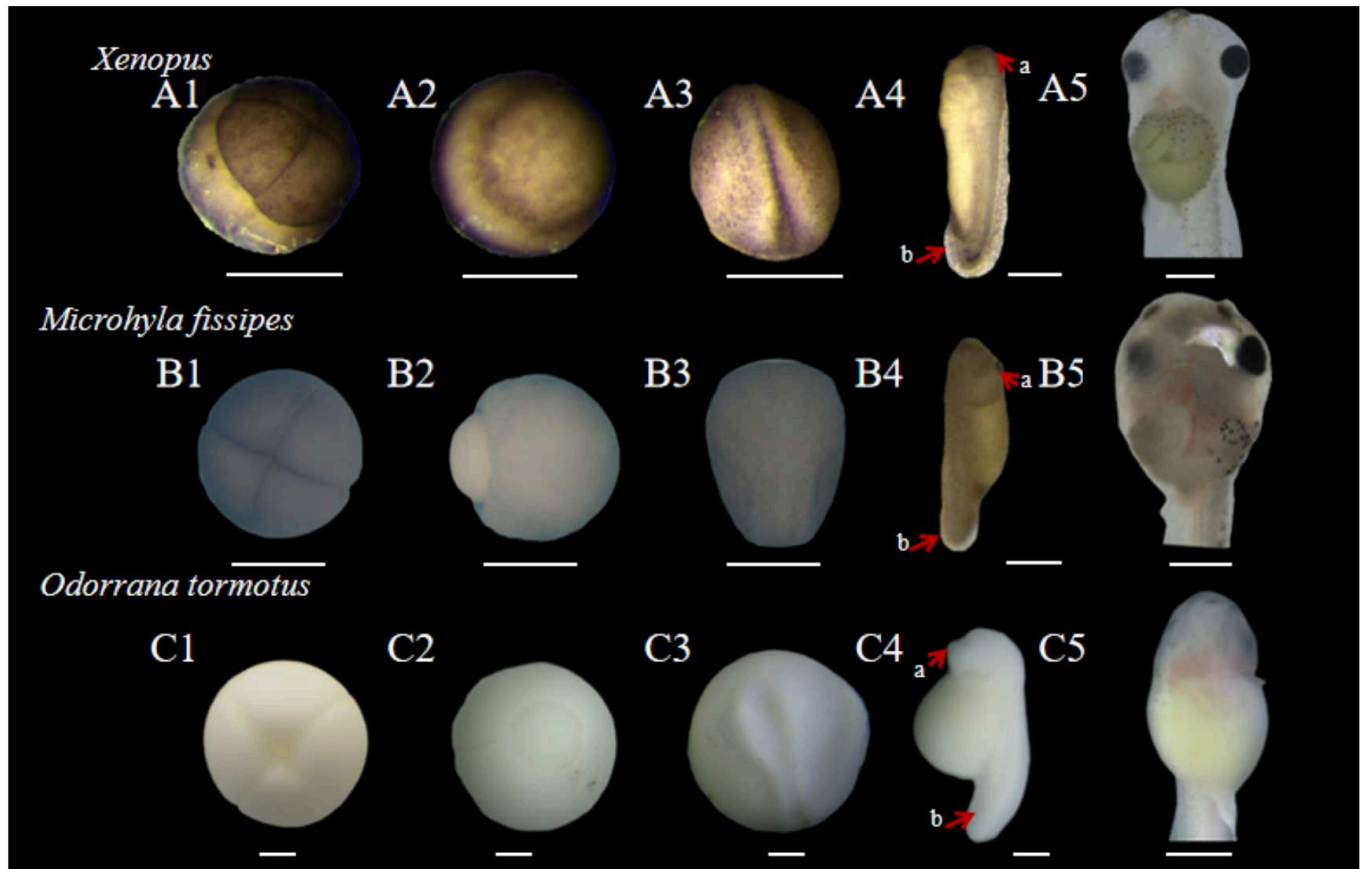


Figure 1

The comparison analysis of representative embryonic developmental stages across 3 species: (A) *Xenopus*, (B) *Microhyla fissipes*, and (C) *Odorrana tormotus*; (A1-C1) Cleavage stages; (A2-C2) Gastrula stage; (A3-C3) Neurula stage; (A4-C4) Tail development; and (A5-C5) Operculum formation. Red arrows (a) show the development of optic vesicles, while red arrows (b) indicate tail bud development. Scale bars are 0.5 mm (A1-C4) and 2 mm (A5-C5).

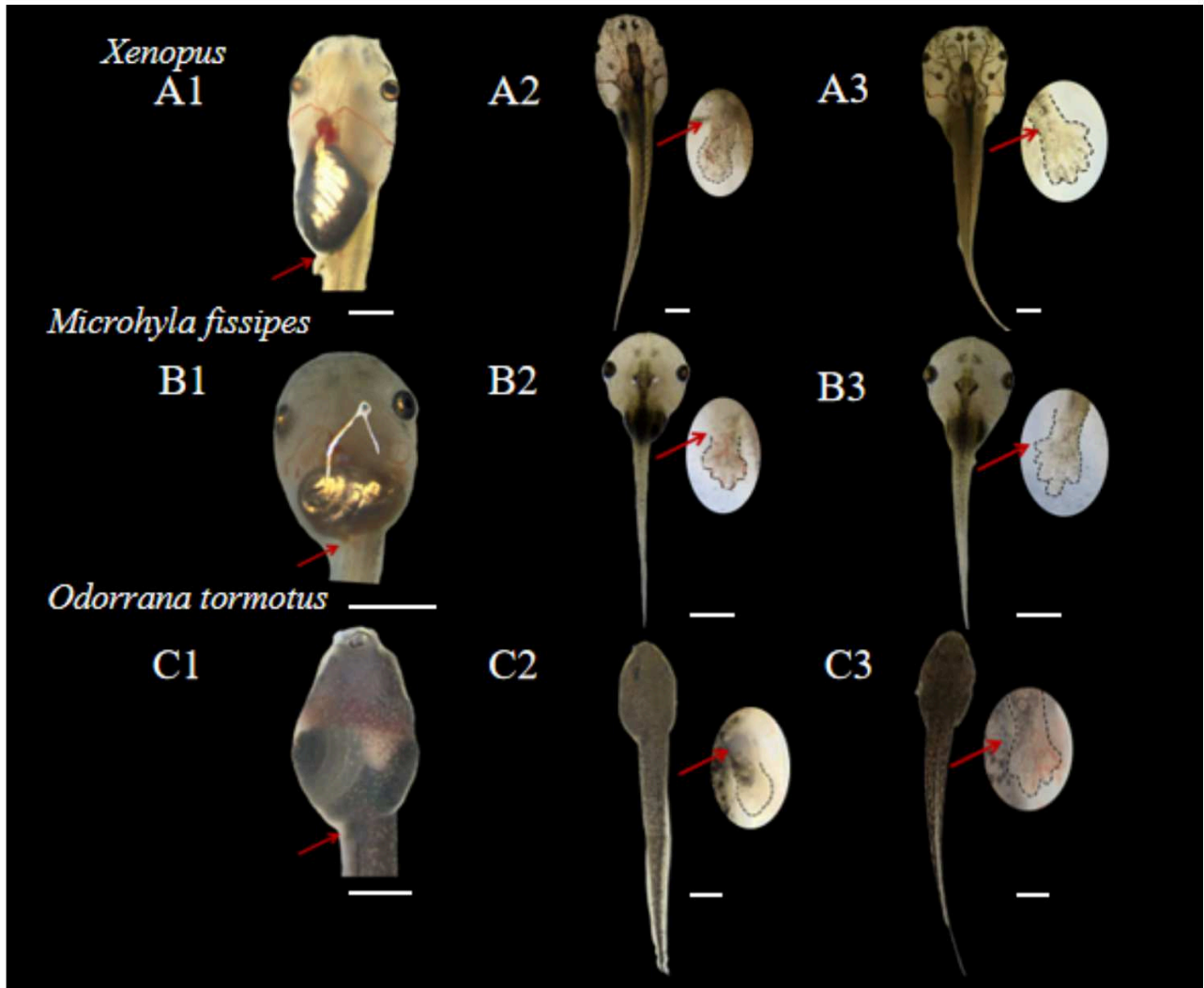


Figure 2

The comparison analysis of representative limb bud developmental stages across 3 species: (A) *Xenopus*, (B) *Microhyla fissipes*, and (C) *Odorrana tormotus*; (A1-C1) Appearance of limb bud; (A2-C2) Development of limb bud; (A3-C3) Toe differentiation. Red arrows show the magnification of limb buds or differentiated toes. Scale bars are 2 mm.

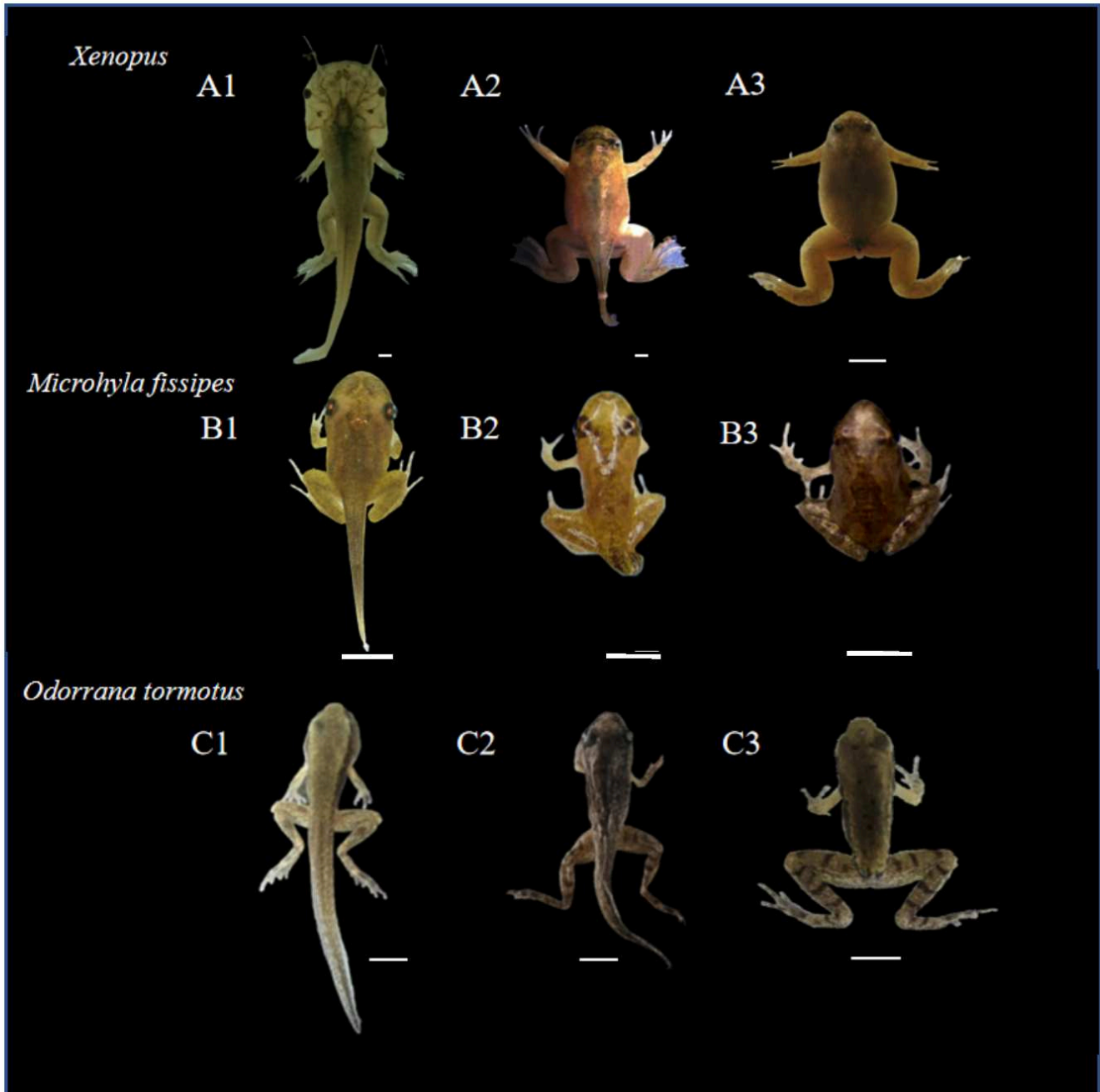


Figure 3

Tail resorption stages in *Xenopus* (A), *Microhyla fissipes* (B), and *Odorrana tormotus* (C). (A1-C1) Eruption of forelimbs (dorsal view); (A2-C2) Tail resorptions at metamorphosis climax (dorsal view); (A3-C3) Completion of metamorphosis (dorsal view). Scale bars are 2 mm.

Supplementary Files

This is a list of supplementary files associated with this preprint. Click to download.

- [Table1.pdf](#)
- [Table2.pdf](#)
- [FigS1.pdf](#)